Atmospheric measurement of point source fossil CO_2 emissions

Jocelyn Turnbull[1,2], Elizabeth D. Keller[1], Troy Baisden[1], Gordon Brailsford[3], Tony Bromley[3], Margaret Norris[1], Albert Zondervan[1]

[1]National Isotope Centre, GNS Science, Lower Hutt, New Zealand
[2]CIRES, University of Colorado at Boulder, Boulder, CO, USA
[3]NIWA, Wellington, New Zealand

Abstract

We use the Kapuni Gas Treatment Plant to examine methodologies for atmospheric monitoring of point source fossil fuel CO_2 (CO_2ff) emissions. The Kapuni plant, located in rural New Zealand, removes CO_2 from locally extracted natural gas and vents that CO_2 to the atmosphere, at a rate of ~0.1 Tg carbon per year. The plant is located in a rural dairy farming area, with no other significant CO_2ff sources nearby, but large, diurnally varying, biospheric CO_2 fluxes from the surrounding highly productive agricultural grassland. We made flask measurements of CO_2 and $^{14}CO_2$ (from which we derive the CO_2ff component) and in situ measurements of CO_2 downwind of the Kapuni plant, using a Helikite to sample transects across the emission plume from the surface up to 100 m above ground level. We also determined the surface CO_2ff content averaged over several weeks from the ^{14}C content of grass samples collected from the surrounding area. We use the WindTrax plume dispersion model to compare the atmospheric observations with the emissions reported by the Kapuni plant, and to determine how well atmospheric measurements can constrain the emissions. The model has difficulty accurately capturing the fluctuations and short-term variability in the Helikite samples, but does quite well in representing the observed CO_2ff in 15 minute averaged surface flask samples and in ~one week integrated CO_2ff averages from grass samples. In this pilot study, we found that using grass samples, the modeled and observed CO_2ff emissions averaged over one week agreed to within 30 %. The results imply that greater verification accuracy may be achieved by including more detailed meteorological observations and refining ^{14}C sampling strategies.

1 Introduction

Emissions of fossil fuel carbon dioxide (CO_2ff) are the main driver of the post-industrial increase in atmosphere CO_2 mole fraction (IPCC, 2007; Tans et al., 1990). Knowledge of the sources and magnitude of CO_2ff emissions is critical to improving our understanding of Earth's carbon cycle and climate system. Large point sources (electricity generation and large-scale industry) make up roughly one third of all CO_2ff emissions (IPCC, 2007). These point sources are the first CO_2ff emissions sector to be regulated under various national and international carbon tax and cap and trade schemes (e.g. Australian Government, 2013; Government of India, 2010). Point sources are also the most likely candidates for emissions reduction by carbon capture and sequestration (IPCC, 2007).

The success of regulatory schemes depends on the ability to demonstrate that emissions targets are actually achieved. Regulating emissions without monitoring "is like dieting without weighing oneself" (Nisbet and Weiss, 2010). Currently, point source emissions are determined using "bottom-up" estimates from self-reported inventory data. Emissions estimates are typically obtained from the volume of fossil fuel (coal, oil or natural gas) consumed and carbon

content of that fuel (Andres et al., 2012; Gurney et al., 2009). Uncertainties in the calculated emissions arise from uncertainties in the amount of fuel used, which may include transcription errors and errors in collating the data, and from uncertainties in the carbon content of the fuels themselves. In some countries, smokestack CO_2 emissions are directly measured (e.g. CEMS in the US), with a likely uncertainty of 20% (Ackerman and Sundquist, 2008). In upcoming regulatory environments, it is also possible that deliberate falsification of reported emissions will occur. Thus there is a need for independent, objective measurements of these emissions both to improve the accuracy of the reported emissions, and to provide independent monitoring as we move into a regulatory environment.

Atmospheric measurements of recently added fossil CO_2 mole fraction can be combined with knowledge of atmospheric transport in a "top-down" approach to infer the CO_2ff emission flux, providing an emission estimate with quantifiable uncertainties, that is independent from the bottom-up approaches. In the top-down approach, two key components are needed: measurements of CO_2ff mole fraction and a model of the atmospheric transport.

CO_2ff cannot be directly measured in the atmosphere, since CO_2ff is but one component of the total CO_2 mole fraction. The CO_2 background mole fraction is ~400 parts per million (ppm) and increasing by 1-2 ppm yr^{-1} primarily due to global CO_2ff emissions (IPCC, 2007; Conway et al., 2011). Large diurnal and seasonal cycles are superimposed on this, mainly due to the seasonally and diurnally varying exchange with the terrestrial biosphere by photosynthesis and respiration as well as biomass burning (IPCC, 2007). Ocean exchange of carbon, although having a gross flux of similar magnitude, is of lesser importance over the land areas where most CO_2ff emissions occur. The CO_2 mole fraction at a given site will also vary with meteorology as different air masses are advected to the location and as vertical mixing varies through time. When the CO_2ff mole fraction added by a point source is large relative to the variability in the CO_2 background, CO_2 measurements alone may be sufficient to determine added CO_2ff mole fraction. However, in many cases, variability in CO_2 background is large relative to the added CO_2ff mole fraction. This is particularly important when there is a strong biospheric carbon flux nearby. Loh et al. (2009) used the WindTrax Lagrangian particle dispersion model to evaluate atmospheric measurements of point source CO_2 and methane emissions at a local scale. They showed that the method could be useful for methane, where the emissions were large relative to the methane background variability, but was more difficult for CO_2, where background variability was a dominant source of uncertainty.

CO_2 derived from fossil sources is entirely free of the isotope ^{14}C, which is removed by radioactive decay with a half-life of 5,730 years (Karlen et al., 1968). All other sources of CO_2 contain ^{14}C at levels close to that of the current atmosphere (Randerson et al., 2002; Turnbull et al., 2009). Thus measurements of the radiocarbon content of CO_2 ($\Delta^{14}CO_2$) can be used to quantify the CO_2ff mole fraction (Suess, 1955; Tans et al., 1979). In the current atmosphere, 1 ppm of added CO_2ff decreases $\Delta^{14}CO_2$ by about 2.6‰ (Turnbull et al., 2009).

$\Delta^{14}CO_2$ can be determined directly from measurements of ^{14}C in CO_2 extracted from flask samples of air (e.g. Turnbull et al., 2007; Graven et al., 2007). The ^{14}C content of CO_2 is also maintained in carbon assimilated by plants so that the average $\Delta^{14}C$ of the assimilated CO_2, and hence the overlying atmosphere at the time of uptake, can be determined from the ^{14}C content

of plant materials (e.g. Hsueh et al., 2007; Palstra et al., 2008). CO_2 assimilation rates vary with local climatic weather conditions, plant type, and plant growth phase, meaning that a complex weighting function may be needed to describe the averaging period (Bozhinova et al., In Press). CO_2 absorption by an alkaline solution (sodium hydroxide, NaOH) is another commonly used method to obtain time-integrated average $\Delta^{14}C$ in the atmosphere (e.g. Levin et al., 2010; Currie et al., 2009; van der Laan et al., 2010).

A number of studies have used correlate tracers to estimate CO_2ff. In this method, a trace gas that is co-emitted with CO_2ff, such as carbon monoxide (CO), is monitored in the atmosphere. If the emission ratio of CO:CO_2ff is known, then CO_2ff can easily be determined (Levin and Karstens, 2007). CO is much more readily measured than $\Delta^{14}CO_2$, so this method can obtain CO_2ff mole fractions at higher spatial and temporal resolution (Vogel et al., 2010; Turnbull et al., 2011a). Unfortunately, the emission ratio CO:CO_2ff is imperfectly known, variable by combustion efficiency and method, and large power plants typically emit little or no CO (USEPA, 2012). Other correlate tracers have been considered, including sulphur hexafluoride (Turnbull et al., 2006), perchloroethylene (Miller et al., 2012), and acetylene (LaFranchi et al., 2013), but most of these tracers are only indirectly associated with CO_2ff combustion sources, so are likely not appropriate for monitoring of individual point source emissions. Further, the amount of correlate trace gases emitted directly from the point source may vary widely depending on the fuel used, combustion process, and "scrubbing" of pollutant gases before they are emitted into the atmosphere. Hence $\Delta^{14}CO_2$ remains the most robust method for quantifying CO_2ff across a range of environments.

Once the CO_2ff mole fraction has been determined, the emission flux can be modeled or estimated by using a description of atmospheric transport from the emission source to the measurement location. This has been performed at various scales using techniques ranging from a simple mass balance model for urban scale emissions (Turnbull et al., 2011a), to a Lagrangian particle dispersion model for the regional scale (Turnbull et al., 2011b), to tracer:tracer flux estimates using radon (Levin et al., 2003; Van der Laan et al, 2010). Modeling studies have demonstrated that long-term trends in regional CO_2ff emissions could be determined from a combination of $\Delta^{14}C$ observations and regional or global modeling (Levin and Rödenbeck, 2007). Monitoring of CO_2ff from point sources has not previously been attempted, but other species emitted by point sources have been monitored in the atmosphere. Mass balance modeling has been successfully used to monitor ozone from large power plants (Trainer et al., 1995; Ryerson et al., 2001). This method uses aircraft sampling at high temporal resolution across transects downwind of the point source, and a simple description of plume dispersion to quantify emissions. It can estimate emissions to within ~50% under consistent wind conditions when emissions are large relative to the background mole fraction. More commonly, Lagrangian atmospheric transport modeling is used to both identify emission sources and to quantify those emissions. Point source emissions of numerous pollutant species have been evaluated using this method, including SO_2, NOx and particulates (e.g. Dresser and Huizer, 2011; Ghannam and El-Fadel, 2013). These studies are focused on air quality impacts, and there is little detailed information about the quality of total flux estimates in the models.

Here we examine methodologies for atmospheric monitoring of point source CO_2ff emissions. Our experimental site is a small, isolated industrial CO_2ff emission source in rural New Zealand. Our focus is on CO_2ff quantification from $\Delta^{14}CO_2$ measurements, examining two different sampling methods: snapshot flask sampling in the atmosphere, and time-integrated sampling from grass. We use a Lagrangian plume dispersion model run forward in time to predict the CO_2ff mole fraction from the known emissions and meteorological data. We then compare the predicted and observed CO_2ff mole fractions to examine the different methods.

Our goal is to evaluate the methods from both scientific and application perspectives, considering:

- Measurement cost and complexity. How easily can the sampling method be deployed at field sites, and how difficult is the measurement?
- What sampling methods are most compatible with the strengths of the current generation of atmospheric transport models? Models imperfectly simulate atmospheric transport, and emissions detection will be more or less robust depending on how the model is used.
- What are the uncertainties in the estimate of the CO_2ff emission flux, and how could these uncertainties be reduced?

2 Methods

2.1 Sampling location and point source description

Our experimental site is the Kapuni Gas Treatment Plant, located in rural New Zealand and run by Vector (figure 1). The Kapuni plant processes natural gas extracted from nearby onshore natural gas wells in the Taranaki Basin. Natural gas from this field contains ~40% CO_2. At the Kapuni plant, the CO_2 is stripped from the natural gas and vented to the atmosphere at a rate of ~0.1 TgC yr^{-1} (NZMED, 2010). This equates to average emissions of about 3,300 gC s^{-1}. The emissions are small relative to many industrial facilities and power plants around the world, for example, the world's largest power plant (Taichung, Taiwan) emits ~300,000 gC s^{-1} (Ummel, 2012; Wheeler and Ummel, 2008). We recognize that there will be differences in applying the results of our study to larger emission sources.

The Kapuni plant is located in a rural dairy farming area, with no other significant CO_2ff sources nearby. The Agri urea plant located 500 m west of the Kapuni plant does emit a small amount of CO_2, but this is approximately 1% of the Kapuni plant emissions (NZMED, 2010). We avoid sampling close to local roads, and also note that traffic counts are low (one vehicle every ~10 minutes), so the overall contribution of traffic CO_2ff in our measurements is expected to be minimal. There is a small CO_2ff source from residential heating using natural gas and from farm vehicle exhaust, but farm and residential power are typically from mains electrical supply with no local CO_2ff emissions. The farmland is highly productive grassland, with large, diurnally varying, biospheric CO_2 fluxes. The surrounding terrain is relatively flat, with elevations within 2 km of the Kapuni plant varying by about 10 m. There are some trees of ~20 m height to the south and west of the plant, and a dip to lower elevation directly to the east where a stream flows (figure 1).

2.2 Sampling methods

2.2.1 Kite platform

A Helikite, a patented combination kite and helium balloon (Allsopp Helikites Ltd, Hampshire, England) was used to sample air from the surface up to 100 m above ground level, downwind of the Kapuni plant, on October 26, 2012. The Helikite was fitted with a GPS (Garmin 60CSx) to determine location at 1 s time resolution. A tethersonde (Graham Digital Design, Amberley, New Zealand) with an anemometer was used to measure wind speed and direction, temperature, and pressure at 10 s resolution. Transmitted data were received at a ground station providing real-time height and wind data. The anemometer cups tangled with the tether line for short periods during the measurement campaign, identified as zero wind speeds; we exclude these periods from our dataset. 300 m of 4 mm OD polyethylene (Leda Extrusions, New Zealand) tubing was attached to the kite tether close to the tethersonde, bringing air from the kite to our mobile lab. A diaphragm pump (KNF, model # N186.1.2KN.18) was placed halfway along the inlet line on the ground to improve flow rate.

The inlet line ran to a cavity ring down spectrometer (CRDS, Picarro model G1301) inside a mobile laboratory. The CRDS provided real-time mole fractions for CO_2 in the air arriving from the intake on the Helikite. Individual observations were made at ~2 s intervals. The measurement precision for CO_2 is better than 0.1 ppm, determined from the spread of repeat measurements of an air standard sampled using an experimental setup similar to that used for this experiment. The CO_2 measurements are referenced to the World Meteorological Organization WMO X2007 CO_2 mole fraction scale to within 0.05 ppm, and one-minute averages of transfer gases have also been determined to a standard deviation on replicates of 0.05 ppm. Methane (CH_4) was simultaneously measured but is not discussed here since CH_4 sources in the area are complex. The transit time from the inlet to the mobile lab was determined from timed puffs of (high CO_2) human breath, and determined as 173 seconds. The flask filling and CO_2 mole fraction measurements are adjusted for this time delay and matched to the GPS and meteorological measurements, which were operating on the same timestamp.

Previously evacuated glass flasks (0.8 – 2 L volume) were filled by opening a valve directly upstream of the CRDS unit without reducing sample flow to the CRDS. The air was dried using magnesium perchlorate and then passed through a diaphragm pump to fill the flasks to a pressure of 2 bar absolute. Flask fill times varied from 2 to 6 minutes, depending on the flask volume. We determine the CO_2 mole fraction in the flask sample as a weighted average of the CO_2 mole fraction measured on the CRDS made during the flask filling time. The weighting function for the flask fill was obtained by logging the pressure increase in a flask, as a function of time, for the flask sampling pump (KNF, model N814KNE) and scaling the resulting function by flask size. The weighting function was then approximated by fitting a polynomial to the pressure change through time, which approximates the fill rate well (r^2=0.99).

2.2.2 Surface flasks

Five surface samplers were also deployed on October 26, 2012 at one location upwind of the Kapuni plant and four locations downwind and beneath the Helikite track. For each sampler, the air is drawn in through an inlet line (6 mm OD, polyethylene) from an intake 3 m off the ground. A deflated 4 L Tedlar bag is slowly filled at a designated flow rate from a manifold operating at a preset overpressure. In this case, three liters of air was collected over 15 minutes. Each sampler was pre-programmed to purge the sample lines for one minute and then collect a 15 minute sample once every 18 minutes. After sampling was complete, a small aliquot was

used to determine the CO_2 mole fraction on the CRDS, and then the air sample was transferred into a pre-evacuated glass flask using the flask pump and pressurization method described above. A subset of these surface samples were selected for $\Delta^{14}CO_2$ analysis.

2.2.3 Grass samples

When plants photosynthesize CO_2, the $^{14}C/^{12}C$ ratio of that CO_2 is altered only by isotopic fractionation during photosynthesis (Suess et al., 1955). The $^{14}C/^{12}C$ fractionation can be quantified from the $^{13}C/^{12}C$ fractionation ($\delta^{13}C$), and $\Delta^{14}C$ for CO_2 and plant material is normalized to a $\delta^{13}C$ of -25‰ (Stuiver and Polach, 1977). Thus the $\Delta^{14}C$ of the plant material can be considered identical to the photosynthesized CO_2, integrated over the period of plant growth.

A number of studies have shown that plant material records the broad spatial patterns of $\Delta^{14}CO_2$ in the modern atmosphere, using corn leaves (Hsueh et al., 2007; Riley et al., 2008), wine ethanol (Palstra et al., 2008), and rice grains (Shibata et al., 2005). Several of these studies compared the observations with model predictions, and achieved reasonable agreement at the continental and regional scales, mostly reflecting the spatial pattern of CO_2ff emissions. However, the exact $\Delta^{14}C$ measured will depend on the growth period of the plant, variations in photosynthetic uptake during the growth period (e.g. weather conditions) and how the plant allocates the photosynthesized carbon among different parts of the plant (Bozhinova et al., in press). The resulting sample integrates over variable rates of photosynthesis but can generally be viewed as an integrator of the daytime photoperiod $\Delta^{14}CO_2$.

We collected samples of grass from farmland around the Kapuni plant on August 15, 2012 and October 24, 2012. The grass species was not specifically identified for these samples, but the dominant species in South Taranaki is a ryegrass, *Lolium perenne* (Roberts and Thomson, 1984). The farmland in this region is divided into small paddocks (fenced fields) and each paddock is grazed by the dairy cow herd for one day every 18-25 days. The grass grows ~20 cm during the regrowth period, and regrazing occurs before any flowering has begun. We sampled grass from paddocks that had been grazed one to two weeks previously, so our samples likely represent an average over one to two weeks. We collected samples of the ~20 cm regrowth, and radiocarbon measurement was performed on part of an individual grass leaf from each sample. As all growth is in the vegetative phase, allocation of carbon to the leaves is likely consistent across the growth period, but there will be some variability in uptake with weather patterns, which we do not account for. We make the simplifying assumption that the leaf samples represent the daytime average for the one-week period preceding sampling. Sample locations were determined using a handheld GPS, and locations close to obstructions such as hedges and buildings were avoided, as were sites close to roads.

2.3 ^{14}C measurement and CO_2ff determination

CO_2 was cryogenically extracted from the flask samples by slowly flowing the air over a Russian doll type liquid nitrogen trap (Brenninkmeijer and Röckmann, 1996). In the case of grass samples, pieces of grass were acid washed (0.5 M HCl at 85°C for 30 minutes) to remove any adhering material, then rinsed to neutral and freeze dried, prior to sealed tube combustion with copper oxide and silver wire at 900°C. The resulting CO_2 was cryogenically purified. CO_2 from either sample type was then reduced to graphite with hydrogen over an iron catalyst,

using methods adapted from Turnbull et al. (2007). The ^{14}C content was measured using accelerator mass spectrometry at GNS Science (Baisden et al., 2013).

Measurement uncertainty in each sample was derived from three sources: counting error of ^{14}C atoms in the sample, counting error in the standards used for calibration, and additional variability amongst those standards. While counting errors in the measurement process are governed by Poisson statistics, we regard the variability in excess of counting errors as being representative of an additional source of uncertainty in the measurement and/or sample preparation. Since these three error sources are assumed independent, they are added in quadrature. All samples in each experimental dataset (two grass sampling experiments, and one flask experiment) were measured in the same AMS measurement wheel. Therefore, we do not include additional uncertainty due to wheel-to-wheel scatter in secondary standards (Turnbull et al., 2007; Graven et al., 2007). The grass samples were measured to 1,000,000 ^{14}C counts or until the graphite target was exhausted, resulting in overall, single sample precision of 1.1 – 1.5‰. Anticipating large CO_2ff contributions in the flask samples, they were counted to 650,000 counts or until the graphite target was exhausted. This, combined with poorer AMS stability during the flask sample wheel measurement (as derived from the scatter of the calibration standards), resulted in overall uncertainties of 2.0 – 2.5‰. Between 4 and 10 secondary standards were also measured in each wheel, and the scatter of these secondary standards within each wheel is, in all cases, consistent with their assigned uncertainties.

Results are reported as $\Delta^{14}C$, the deviation of the sample ^{14}C content from that of the absolute radiocarbon standard, and corrected for radioactive decay since time of collection and normalized to a $\delta^{13}C$ of -25‰ (Stuiver and Polach, 1977). CO_2ff is determined from the $\Delta^{14}C$ of the grass or flask sample, taking advantage of the fact that CO_2ff contains zero ^{14}C ($\Delta^{14}C$ = -1000‰), whereas all other CO_2 sources have $\Delta^{14}C$ values close to that of the atmosphere. The CO_2ff added relative to a clean air background measurement can be determined using mass balance (Levin et al., 2003).

When the CO_2 content of the observed sample is known, as for our flask samples, CO_2ff is calculated from

$$CO_2ff = \frac{CO_{2obs}\left(\Delta_{obs} - \Delta_{bg}\right)}{\Delta_{ff} - \Delta_{bg}} - \beta \quad \text{(eqn 1)}$$

following equation 3 in Turnbull et al. (2009). CO_2obs is the CO_2 mole fraction in the observed sample, and Δ_{obs} and Δ_{bg} are the $\Delta^{14}C$ of the observed sample and background sample, respectively. Δ_{ff} is the $\Delta^{14}C$ of CO_2ff, and is assigned to be -1000‰. Δ_{bg} for the flask samples was determined from surface flasks collected upwind of the Kapuni plant (figure 1) on the same day, at about the same time of day.

β is a small correction term to account for the fact that the $\Delta^{14}C$ of CO_2 from other sources may be slightly different from that of the atmosphere, and may include contributions from heterotrophic respiration, oceanic CO_2 sources, and nuclear-industry-produced ^{14}C. Here, we set β to zero, and justify this choice for each possible contribution. The background sample was collected close to our observational sampling sites in both space and time, so that at our site a few tens of kilometers from the ocean, it is likely that ocean CO_2 exchange has altered $\Delta^{14}C$,

but this alteration occurred in both background and observed samples. There is no nuclear industry activity in New Zealand and only a handful of reactors elsewhere in the Southern Hemisphere (Graven and Gruber, 2011), so we assume there is no nuclear industry bias in our samples. Of most importance is the effect of heterotrophic respiration occurring throughout the landscape. This is expected to have equally impacted both background and observed $\Delta^{14}C$, and hence the heterotrophic respiration correction is implicitly included in the background. We tested how important this assumption might be, using the Biome-BGC model v4.2 (Thornton et al., 2002; Thornton et al., 2005), calibrated to New Zealand pasture (Baisden and Keller, 2013). The Biome-BGC model is an ecosystem process model that simulates the biological and physical processes controlling cycles of carbon, nitrogen and water of vegetation and soil in terrestrial ecosystems. Important inputs include weather conditions at a daily time step and site-specific information such as elevation, soil composition and rooting depth. The model has a set of 43 ecological parameters that can be customized for a particular ecosystem. In previous work, using pasture clipping data from several sites distributed across New Zealand, we adjusted selected model parameters to fit modeled pasture growth to the data to obtain a national model of pasture production for both dairy and sheep/beef pasture at a grid scale of ~5 km (Keller et al., in review). We ran the dairy model for the grid location that includes the Kapuni processing plant to arrive at an estimate for the respiration CO_2 flux and its $\Delta^{14}C$ at the sampling sites. We assume a boundary layer flushing time of one day at our site, and using the Biome-BGC estimates, β due to the heterotrophic respiration flux could be 0.2-0.4 ppm. This is the maximum bias if the heterotrophic respiration flux occurs at the observation site but not in the background, an unlikely scenario.

In the case of the grass samples, the CO_2 content of the sampled air is unknown, so CO_2ff was calculated using the slightly different formulation reported as equation 6 in Turnbull et al. (2009), which requires that the CO_2 of the background air (CO_2bg) be known.

$$CO_{2ff} = \frac{CO_{2bg}\left(\Delta_{obs} - \Delta_{bg}\right)}{\Delta_{ff} - \Delta_{obs}} - \beta' \quad \text{(eqn 2)}$$

The grass Δ_{bg} values were from samples collected ~20 km to the north of the Kapuni plant in similar dairy farmland, on the same day as the observed samples were collected. The background CO_2 mole fraction was estimated as 390 ppm, from measured values at Baring Head, New Zealand at the same time (Currie et al., 2009; dataset extended to 2012). A 4 ppm error in the choice of CO_2 observed (eqn 1) or background (eqn 2) value equates to a 1% error in the determined CO_2ff mole fraction, small relative to the measurement and atmospheric transport uncertainties. β' is also a bias correction, formulated slightly differently to β, but accounting for the same biases. We also set this value to zero.

A further very small bias is induced by the $\delta^{13}C$ normalization in the calculation of $\Delta^{14}C$, since the $\delta^{13}C$ of CO_2ff is different from that of the atmosphere (Vogel et al., 2013). In our case, this is of minimal importance, since the CO_2ff from Kapuni is -13.8‰ (measured in our laboratory using CO_2 supplied by the Vector Kapuni plant), quite close to that of the atmosphere. This implies an overestimate of CO_2ff of 1 - 2 %, less than 0.1 ppm for most of our measurements. We ignore this bias, as $\delta^{13}C$ was not measured on these samples, and in fact, the atmospheric $\delta^{13}C$ value cannot be easily determined from the grass samples since isotopic fractionation

occurs during assimilation of CO_2 into the plant. Note that although ^{14}C fractionation also occurs during assimilation, this is corrected for mathematically in the $\Delta^{14}C$ notation.

2.4 Atmospheric transport model

WindTrax (Thunder Beach Scientific, Nanaimo, Canada) is a Lagrangian stochastic particle dispersion model, designed for modeling short-range atmospheric dispersion (horizontal distances of less than 1 km from source). The physics is described by Flesch et al. (2004) and Wilson and Sawford (1996). We run the model in forward mode, in which CO_2ff emissions are assumed known and gas concentrations or mole fractions at any given location are unknowns to be determined. We set the model to release 10^5 particles from the simulated stack at every time step, enough to reduce model uncertainty to satisfactory levels (the more particles released, the lower the uncertainty in model predictions). Each particle is transported according to the model physics and specified meteorological conditions. Concentration sensors are placed at the observation locations, and the model outputs a prediction of CO_2ff mole fraction at each sensor for each time step. The wind speed and direction (along with other atmospheric conditions), combined with the prescribed emission rate, determine the predicted CO_2ff mole fraction at that location and time. We then compare the model prediction with the observed mole fractions. Alternatively, the model can be run in backward mode to predict the emissions from the observed CO_2ff mole fractions, but this is computationally more expensive, and forward mode allows us to also investigate the broader patterns of the predicted plume dispersion. The model is stochastic, not deterministic, so the outcome of model runs will vary even with the same initial conditions and parameters. This is a source of model error that is quantified at each time step. The terrain elevation varies by about 10 m across our sampling area, and this is not accounted for in our model simulations.

Daily emissions were provided by the Kapuni plant operator, Vector (P. Stephenson, personal communication). We assume constant emissions for each 24-hour period, although Vector estimates that emission rates may vary by up to 3% during that time. Emission rates were 3,100 – 3,750 gC s^{-1} in the two weeks of August 2012 preceding the day when the first grass samples were collected, 2,700 – 3,500 gC s^{-1} during the two weeks prior to grass sample collection on October 25, 2012, and 3,200 gCs^{-1} on October 26, 2012 when the flask samples were collected. Emissions are from two stacks, both 35 m high, and ~10 m apart. In the model, we assume that the stacks are close enough in space to be modeled as a single point source. We release the emissions from the known stack height of 35 m above ground level. We also tested an alternative scenario where emissions were released from a height of 45 m above ground level, 10 m higher than the actual stack height, to account for buoyant rise of the warm, moving plume (Briggs, 1975). This value was determined using the known emission temperature (80-85 °C) and stack diameter (0.6 m), and a velocity estimated from the CO_2 emission rate. Under the unstable atmospheric conditions during our measurement campaigns, the difference in effective stack height did not make a significant difference in our results.

For the flask samples, we use a model time step of approximately 10 s, commensurate with the wind data collected from the Helikite at 10 s resolution and fed into the model. We note that previous studies have shown that WindTrax performs best over much longer averaging periods (Flesch et el., 2004), on the order of 10 – 30 minutes, and using the model with very short time intervals (i.e. less than 1 min) is problematic, as the relationships built into the model assume atmospheric equilibrium, which might not be the case at such short time scales. Our results

should be interpreted with caution, as they might reflect the inability of the model to resolve atmospheric instability and rapid fluctuations at such fine time scales.

In the case of the grass samples, 10-minute time steps were used with wind data from the stationary meteorological station installed close to the site (figure 1). Wind information was not available from the local site for the August grass growth period. Instead, we used the meteorological data obtained for the week directly following the grass sampling. We justify this by comparing data from the two weeks at a long-term station ~20 km away in Hawera, which provides hourly temperature and pressure data. This long-term station data could not be used as a proxy for wind speed and direction at our Kapuni site because the particular locations and orientations of the two sites relative to Mt Taranaki result in large differences in wind direction between the two sites. However, we found that the weeks preceding and following our August grass sampling had similar wind patterns at Hawera.

In the absence of detailed measurements of turbulence and atmospheric stability, a general stability category was specified in WindTrax using the Pasquill-Gifford classes (Pasquill, 1961; Gifford, 1961). The Monin-Obukhov length L (a meteorological measurement of stability) was then calculated by the model along with other related variables. As the measurements necessary for a more exact quantification were not made, we assumed 'slightly unstable' conditions for the flask samples, and 'moderately unstable' conditions for the grass sampling. The meteorological conditions during the grass sampling periods may more correctly match neutral to slightly unstable conditions, but we found that under these conditions, the model underestimated the observed plume dispersion. This is discussed further in section 4.2.

The model output was sampled at the location and corresponding time step(s) for each sample. As the Helikite moved during the flask filling procedure, the modeled sensor was moved both horizontally and vertically according to the location obtained from the GPS on the kite. For the simulation with the grass samples, the model was sampled at the GPS location and 1.5m above ground level to avoid surface effects. We found that grouping several model sensors around the GPS location and then averaging their output was more accurate than using just one. In all results reported for the grass samples, we used four sensors placed at the corners of a square 30.5 x 30.5 m, with the actual sample location in the center. The model output was averaged over all daytime time steps for the week prior to grass sampling to arrive at a final predicted CO_2ff mole fraction.

3 Observational Results

3.1 CO_2 measurements

During the Helikite sampling period on October 26th, 2013, the measured CO_2 mole fraction varied from 360 ppm at ground level to 592 ppm in samples within the Kapuni emission plume (figures 2 and 3). The emission plume moved during the four-hour sampling period, so that our Helikite observed the plume at different locations across the north-south transect at different times. The plume also moved in the vertical, and was more dispersed at some times than at others.

In figure 3, strong photosynthetic drawdown can be seen in the ~7 m above the surface, with CO_2 mole fractions as low as 360 ppm, about 30 ppm of drawdown. Above 7 m, the CO_2

451 background can be estimated from the lowest CO_2 mole fractions observed (figure 3). This
452 background varied from 390 – 395 ppm with height, and also evolved during the four-hour
453 measurement time. CO_2 mole fraction in the upwind surface flask samples (collected three
454 meters above ground) varied from 386.3 to 387.4 ppm over the 4 hr measurement period.
455
456 We determine the CO_2 enhancement over background (ΔCO_2) in each CRDS or flask sample
457 by subtracting the estimated height-dependent CO_2 background value (figure 3) from the
458 observed CO_2 mole fraction. In this method, uncertainty in the background mole fraction
459 propagates directly to uncertainty in the CO_2 enhancement. The CO_2 measurement uncertainty
460 is small relative to the background uncertainty, so the total uncertainty in the enhancement for
461 this dataset is determined from the range of background CO_2 values, and is ± 15 ppm in the
462 lowest 7 m, and ± 2.5 ppm above 7 m. This level of uncertainty is quite significant for most of
463 the measurements, except those where the enhancements are very large. The median CO_2 mole
464 fraction for samples taken above 7 m was 397 ppm, so that the majority of measurements are
465 difficult to distinguish from the CO_2 background of 390 - 395 ppm.
466
467 *3.2 CO_2 and CO_2ff from ^{14}C in flasks*
468 CO_2ff in the flask samples ranged from 0.6 to 52 ppm, with one-sigma uncertainties of 1.3 ppm
469 (figure 4). Background $\Delta^{14}C$ is not changed by CO_2 drawdown, and hence was less variable
470 than background CO_2. Δ_{bg} varied from 39.2 ± 2.6 to 43.9 ± 2.8 ‰, (using Student's t-test,
471 these values do not differ significantly, p = 0.39).
472
473 We compare the ^{14}C-derived CO_2ff with ΔCO_2 using the ratio ΔCO_2:CO_2ff ($R_{CO2:CO2ff}$) (figure
474 5). If the CO_2 emitted from the Kapuni plant is entirely fossil-derived, then ΔCO_2 should be
475 equal to CO_2ff, and $R_{CO2:CO2ff}$ equal to one. We find that for the 15 Helikite samples, $R_{CO2:CO2ff}$
476 = 1.3 ± 0.4 ppm/ppm, suggesting that there may be a contribution of non-fossil CO_2 in the
477 Kapuni emission plume. However, when we increase the CO_2 background values by 3 ppm
478 (within the range of background variability), we find $R_{CO2:CO2ff}$ = 1.0 ± 0.3 ppm/ppm (blue
479 points in figure 5), indicating that the plume CO_2 is entirely fossil derived. The variability in
480 $R_{CO2:CO2ff}$ is therefore likely predominantly due to uncertainties in determining the flask ΔCO_2
481 and background CO_2, and also to uncertainties in CO_2ff which are important in the lower mole
482 fraction samples. The emitted plume appears to be entirely fossil-derived, within the
483 uncertainties of our measurements.
484
485 *3.3 CO_2ff from grass samples*
486 The derived CO_2ff in the grass samples for the two sampling dates of August 14th and October
487 24th, 2012 are shown in figure 6. Grass samples were measured to $\Delta^{14}C$ precision of 1.1 to
488 1.5 ‰. This equates to 0.6 to 0.7 ppm uncertainty in CO_2ff.
489
490 CO_2ff mole fraction derived from the grass samples varies from 0.4 to 3.9 ppm in the August
491 samples, and -0.2 to 17.0 ppm in the October samples. A negative CO_2ff value is non-physical,
492 but -0.2 ppm is within one sigma of zero. The highest CO_2ff values were observed in areas
493 that were most consistently downwind of the plant, and locations closer to the plant typically
494 had higher CO_2ff values (figure 6). In August, the wind direction was somewhat variable,
495 dominantly bringing the plume to the east or south of the plant, but sites to the northwest were
496 also occasionally downwind, resulting in small CO_2ff values at all these locations. In October,

the winds were consistently from the west, resulting in larger enhancements to the east of the Kapuni plant than in the August samples, and no CO_2ff detected in the sample to the northwest.

4 Comparison of observation and model CO_2ff

4.1 Kite and surface flask samples

The model predicts CO_2ff in the Helikite and surface flask samples of 0 to 19.1 ppm. The model results for the kite samples are generally lower than the observed CO_2ff (figure 7), except for a few samples where observed CO_2ff was quite small. Other work shows that small errors in the simulated wind direction can result in large errors in the modeled CO_2ff mole fraction for individual samples (Dresser and Huizer, 2011). Thus the model may frequently miss the location of the plume over short time periods of a few minutes when the wind direction is fluctuating rapidly. We deliberately sampled in the center of the plume in the area of highest mole fraction, and the likelihood of modeling this specific point accurately is low given the error inherent in these types of models. The assumption that the time-averaging interval represents an equilibrium state of the atmosphere is built into the model. However, these conditions are most likely not met in our simulations. As mentioned earlier, WindTrax is known to perform poorly at time resolutions of less than about 10 minutes (Flesch et al, 2004). Our results reflect the bias in our sampling method as well as the model error associated with non-equilibrium conditions over very short time-averaging periods. The agreement is much better for the surface flasks, likely because of the longer averaging period of 15 minutes (figure 8).

4.2 Grass samples

The modeled CO_2ff values for the grass samples are shown in figure 6 and range from 0.4 to 4.9 ppm in the August samples and 0.7 to 17.4 ppm in the October samples. The modeled predictions, like the observations, have the highest CO_2ff values in the dominant wind direction, and samples taken closer to the source have higher modeled CO_2ff (figure 8). However, it can be seen that the model significantly underestimates CO_2ff in a number of the October samples collected to the southeast of the Kapuni plant. In August, the samples were collected from sites surrounding the Kapuni plant in all directions, and the wind direction was more variable, whereas in the October case, the wind direction was consistently from the west (figure 6). Discrepancies at the edge of the plume in the October samples suggest the model is not sufficiently dispersive in the horizontal.

The model simulations assumed moderately unstable atmospheric conditions. We tested the model with neutral and slightly unstable conditions but found that under these conditions, the model was even less dispersive in the horizontal (results not shown). This was most apparent in the October samples, where the slightly unstable model simulation predicted larger CO_2ff in the samples taken directly west of the plant, but very low CO_2ff in the samples taken to the north and south along the same transect shown in figure 1 and figure 6b. We also tested our choice of effective stack height for the emissions (45 m), but found little change in the modeled results, with a significant change in the modeled result for only one of the sampling locations. There was no change overall in the coefficient of determination (r^2) between model and observations.

5 Uncertainty in emissions estimated from comparison of observations and model

We further quantify the comparison between the model and observations for the surface flasks and grass samples and evaluate the model-observation mismatch by determining the ratio CO_2ff_{model}:CO_2ff_{obs} ($R_{model:obs}$) for each individual grass sample, and then calculate the mean $R_{model:obs}$. We also report the one-sigma scatter of the individual $R_{model:obs}$ results. Since the model does a very poor job of simulating the Helikite observed CO_2ff, we exclude these samples from this analysis.

Using all 21 measurements, including the four surface flasks collected on October 26th, 2012, eight grass samples from August 2012, and nine grass samples from October 2012, we find good overall agreement between the model and observations ($r^2 = 0.8$, figure 8). The mean $R_{model:obs} = 0.8 \pm 0.5$. That is, on average, the modeled CO_2ff is 20% lower than the observed CO_2ff, but with significant scatter among the individual measurements. Using the August and October grass samples alone, we find $R_{model:obs}$ of 0.8 ± 0.6. Examining just the August dataset (n=8), we find a less biased but more uncertain agreement between observation and model, with mean $R_{model:obs}$ of 1.0 ± 0.7. The larger scatter on this dataset is mainly because the CO_2ff values are quite small for this dataset. Looking at the October measurements alone, we find a slightly larger underestimate in the model, with $R_{model:obs} = 0.7 \pm 0.3$. In all cases, the model remains within one sigma of a 1:1 match with observations.

To infer the uncertainty in emissions from our study, we tested the model response across a wide range of emission rates, and found that it is, as expected, linear. Thus, if model transport were correct, we would infer from this that the reported emission rate was too low by 30 % in our worst case for the October grass samples. For this experiment, we assume that the reported emissions from the Kapuni plant are correct, and therefore, any differences between the modeled and observed CO_2ff mole fractions must be due to uncertainties in our methods and modeling. Thus we estimate, from our worst case model-observation mismatch that the uncertainty in emissions from our grass sample pilot study is 30 % or better.

6 Discussion and Recommendations

In this pilot study, we found that atmospheric ^{14}C measurements of ~1 week integrated samples could be used to estimate CO_2ff emissions from a point source to 30 % or better. This uncertainty estimate is derived from the comparison of our top-down observations with forward modeling, so incorporates all sources of error, including model transport errors, sampling biases and measurement uncertainties. We now consider those various sources of error, the practicalities of field measurements, and outline some improvements that could substantially improve the method and reduce uncertainties in the near future.

Large CO_2ff mole fractions were observed in the "snapshot" Helikite samples collected over a few minutes, but the WindTrax model was unable to accurately predict the high observed CO_2ff mole fractions. Conversely, the model was quite skillful in predicting the observed CO_2ff mole fractions in the long-term averaged grass samples and in 15 minute averaged surface flasks. The model performed best in capturing the broad spatial pattern of emissions around the Kapuni plant as shown in the August sampling pattern. The model was less skillful at capturing the somewhat finer-scale pattern of the October grass samples, which were predominantly sampled in the same sector. This result is consistent with findings from other studies (e.g. Dresser and Huizer, 2011) that show that small errors in model transport of point

source emissions can result in the emission plume being incorrectly located. Averaging the model results over time can reduce the impact of these errors. This conclusion is likely broadly applicable to local scale plume dispersion models such as WindTrax, as well as to regional scale Lagrangian models. The model skill will likely also be improved by more detailed meteorological measurements, including estimates of boundary layer turbulence and atmospheric stability.

We found the long-term averaged grass sampling better suited to the model skill than the snapshot Helikite flask samples. Grass sampling is also far cheaper and easier than flask sampling, particularly from an elevated platform such as the Helikite. Flask sampling requires flasks and the equipment to fill them, which may run to many thousands of dollars per sampling system. Elevated platforms such as the Helikite, as well as aircraft and unmanned aerial vehicles can also be expensive, can only operate under specific meteorological conditions and may be subject to air traffic regulations. In contrast, plant sampling can be done simply and quickly using only a few plastic bags and a handheld GPS to record locations. Whereas flask samples may be limited in size by the practicalities of flask volumes and pumping rates, large plant material samples can be collected to facilitate replicate measurements if required. Plant sampling is also less intrusive and less visible to the power plant operators and the public, which may be advantageous in some situations. The laboratory ^{14}C preparation, while slightly different for each sample type, is of similar complexity and cost. However, plant sampling may suffer biases that cannot be easily quantified. The particular environment at our Kapuni site is conducive to the grass sampling method, with rapid grass growth and regular grazing to consistently remove old growth before flowering. Biases in the $\Delta^{14}C$ of grass or other plant material due to the details of plant CO_2 assimilation through time may make this method challenging in other locations. In future work, we will examine alternative integrated sampling techniques such as NaOH absorption that provide a similar integration period, but allow more control over when CO_2 is collected.. This type of sampler would require more complex field sampling than plant material, but could still be relatively easily deployed in the field, allows collection of large amounts of CO_2, and laboratory methods are well-established.

Uncertainties in observed CO_2ff for the grass samples come from the ^{14}C measurement uncertainty, uncertainties in the CO_2 assimilation period represented by the grass sample, and from the choice of background. Large gains in ^{14}C measurement uncertainty are unlikely in the near future, but the impact of measurement uncertainties could be reduced by measuring multiple aliquots of each sample, or preferably by collecting and measuring more samples at higher spatial and temporal resolutions to obtain a greater data resolution for the model – observation comparison. As already discussed, uncertainties in the CO_2 assimilation period could be reduced by using an alternative integrated sampling technique such as NaOH absorption. We prepared and measured an individual grass leaf from each sample, but homogenizing and measuring a mixture of several leaves, possibly from several grass plants, might give a more representative sample. There is also potential for bias in observed CO_2ff from the choice of background. We used a single background measurement for each dataset, and any bias in that background will result in a consistent bias in $R_{model:obs}$ calculated for each sample. Making several background measurements would reduce background uncertainty and bias.

The Kapuni plant emissions are quite small (two orders of magnitude) relative to many fossil fuel power plants around the world. Larger point sources will produce larger observed CO_2ff mole fractions, and hence relatively smaller measurement uncertainties. However, many large power plants will have much higher stack emission heights of 100 to 800 m, and plume buoyancy due to hot emissions might raise the effective emission height even further. Therefore surface or near-surface measurements might need to be made further downwind to observe the plume. At these larger distances from the source, the plume will be more dispersed and hence observed CO_2ff mole fractions will be reduced, likely to similar magnitude to those we observed at Kapuni. A further modeling consideration is that in this study we used only daytime measurements. It is well-known that atmospheric transport models perform best in the mid-afternoon when the boundary layer is well-mixed, but have difficulty in accurately representing the nocturnal boundary layer. Thus most researchers utilize only daytime measurements. This represents an unresolved difficulty in assessing overall emissions for power plants, which may have significant diurnal variability in their emission rates.

We deliberately selected a location with reasonably flat terrain where atmospheric transport is straightforward. More complex terrain will make the transport modeling more difficult and will require additional care in selection of optimal sampling locations and times. Extending this work to sites with multiple emission sources will also complicate interpretation.

From this pilot experiment, we believe that it is realistic to substantially reduce the uncertainty in atmospheric determination of point source CO_2ff emissions in the near future. A goal of 10-20% overall uncertainty appears realistic.

7 Acknowledgements

This work was funded by GNS Science Strategic Development Fund and public research funding from the Government of New Zealand. Jenny Dahl, Kelly Lyons and Johannes Kaiser assisted with ^{14}C measurements. Ross Martin assisted with analyzing the vertical profile data from the Helikite radiosonde. We wish to thank Peter Stephenson and the staff at the Vector Kapuni processing plant providing necessary details on the plant's CO_2 emissions and their interest in the research. Darryl and Alison Smith, Roger Luscombe, Brent and Kevin Parrett all generously allowed us access to their land for sampling and provided helpful information on local conditions. Thanks to the two reviewers, Zoe Loh and Felix Vogel, for their thoughtful comments and suggestions.

8 Figure captions

Figure 1. Map showing location of Kapuni processing plant and kite sampling locations.

Figure 2. Measured CO_2 mole fraction across transect from south to north. Large black circles indicate the flask sampling locations.

Figure 3. Measured CO_2 mole fraction as a function of altitude. Colours indicate the time of day.

Figure 4. CO_2ff calculated from flask samples from the Helikite and surface flasks on October 26th, 2013.

Figure 5. $R_{CO2:CO2ff}$ in each flask sample. Blue points use the assigned CO_2 background values, red points apply a 3 ppm bias to the CO_2 background values in calculating $R_{CO2:CO2ff}$.

Figure 6. CO_2ff in grass samples collected on August 14th, 2012 (top) and October 24th, 2012 (bottom). The observed CO_2ff derived from $\Delta^{14}C$ is shown in yellow, and the modeled CO_2ff prediction is shown in white. Markers indicate the exact sampling location. A wind rose showing the direction of the wind patterns over the previous one-week period is inset (bars indicate the direction the wind is traveling to). In the lower panel the point indicated with the arrow was measured 500 m to the north-west, off the map.

Figure 7. Observed CO_2ff versus modeled CO_2ff for the kite (red) and surface (grey) flask samples. Error bars are omitted for clarity.

Figure 8. Comparison of observed and modeled CO_2ff from the August (red) and October (blue) grass samples, and October 26th surface flasks (grey). The 1:1 line is shown in black.

9 References

Ackerman, K. V., and Sundquist, E. T.: Comparison of two US power-plant carbon dioxide emissions data sets, Environmental Science & Technology, 42, 5688-5693, 2008.

Andres, R. J., Boden, T. A., Bréon, F. M., Ciais, P., Davis, S., Erickson, D., Gregg, J. S., Jacobson, A., Marland, G., Miller, J., Oda, T., Olivier, J. G. J., Raupach, M. R., Rayner, P., and Treanton, K.: A synthesis of carbon dioxide emissions from fossil-fuel combustion, Biogeosciences, 9, 1845-1871, 10.5194/bg-9-1845-2012, 2012.

Australian Government: Starting emissions trading on 1 July 2014, Canberra, Australia, 2013.

Baisden, W. T., and Keller, E. D.: Synthetic Constraint of Soil C dynamics Using 50 Years of Radiocarbon and Net Primary Production (NPP) in a New Zealand Grassland Site, Radiocarbon, 55, 1071-1076, 2013.

Baisden, W. T., Prior, C. A., Chambers, D., Canessa, S., Phillips, A., Bertrand, C., Zondervan, A., and Turnbull, J. C.: Radiocarbon sample preparation and data flow at Rafter: Accommodating enhanced throughput and precision, Nuclear Instruments and Methods, B294, 194-198, 2013.

Bozhinova, D., Combe, M., Palstra, S. W. L., Meijer, H. A. J., Krol, M. C., and Peters, W.: The importance of crop growth modeling to interpret the $^{14}CO_2$ signature of annual plants, Global Biogeochem. Cycles, 27, 792-803, doi:10.1002/gbc.20065, 2013.

Brenninkmeijer, C. A. M., and Röckmann, T.: Russian doll type cryogenic traps: improved design and isotope separation effects, Analytical Chemistry, 68, 3050-3053, 10.1021/ac960208w, 1996.

Briggs, G.: Plume Rise Predictions, in: Lectures on Air Pollution and Environmental Impact Analysis, American Meteorological Society, Boston, Massachusetts, 59-111, 1975.

Conway, T. J., Lang, P. M., and Masarie, K. A.: Atmospheric carbon dioxide dry air mole fractions from the NOAA/ESRL Carbon Cycle Global Cooperative Network, 1968-2010, version 2011-06-21, Path: ftp://ftp.cmdl.noaa.gov/ccg/co2/flask/event/, 2011.

Currie, K. I., Brailsford, G., Nichol, S., Gomez, A., Sparks, R., Lassey, K. R., and Riedel, K.: Tropospheric $^{14}CO_2$ at Wellington, New Zealand: the world's longest record, Biogeochemistry, 104, 5-22, 10.1007/s10533-009-9352-6, 2009.

Dresser, A. L., and Huizer, R. D.: CALPUFF and AERMOD Model Validation Study in the Near Field: Martins Creek Revisited, Journal of the Air & Waste Management Association, 61, 647-659, 10.3155/1047-3289.61.6.647, 2011.

Flesch, T. K., Wilson, J. D., Harper, L., Crenna, B., and Sharpe, R.: Deducing ground-to-air emissions from observed trace gas concentrations: A field trial, journal of applied meteorology, 43, 487-502, 2004.

Ghannam, K., and El-Fadel, M.: Emissions characterization and regulatory compliance at an industrial complex: An integrated MM5/CALPUFF approach, Atm. Env., 69, 156-169, 10.1016/j.atmosenv.2012.12.022, 2013.

Gifford, F. A.: Use of Routine Meteorological Observations for Estimating Atmospheric Dispersion, Nuclear Safety, 2, 47-57, 1961.

Government of India: India: Taking on Climate Change Post-Copenhagen domestic actions, Ministry of Environment and Forests, New Delhi, 2010.

Graven, H. D., and Gruber, N.: Continental-scale enrichment of atmospheric $^{14}CO_2$ from the nuclear power industry: potential impact on the estimation of fossil fuel-derived CO_2, Atmos. Chem. Phys., 11, 12339-12349, 10.5194/acp-11-12339-2011, 2011.

Graven, H. D., Guilderson, T. P., and Keeling, R. F.: Methods for high-precision ^{14}C AMS measurements of atmospheric CO_2 at LLNL, Radiocarbon, 49, 349-356, 2007.
Gurney, K. R., Mendoza, D. L., Zhou, Y., Fischer, M. L., Miller, C. C., Geethakumar, S., and de la Rue du Can, S.: High resolution fossil fuel combustion CO_2 emission fluxes for the United States, Environmental Science and Technology, 43, 5535-5541, 2009.
Hsueh, D. Y., Krakauer, N. Y., Randerson, J. T., Xu, X., Trumbore, S. E., and Southon, J. R.: Regional patterns of radiocarbon and fossil fuel-derived CO_2 in surface air across North America, Geophys. Res. Lett., 34, L02816, 10.1029/2006gl027032, 2007.
Karlen, I., Olsson, I. U., Kllburg, P., and Kilici, S.: Absolute determination of the activity of two ^{14}C dating standards, Arkiv Geofysik, 4, 465-471, 1968.
Keller, E. D., Baisden, W. T., Timar, L., Mullan, B., and Clark, A.: Adapting the Biome-BGC Model to New Zealand Pastoral Agriculture, Env. Softw. Mod., in review.
LaFranchi, B. W., Pétron, G., Miller, J. B., Lehman, S. J., Andrews, A. E., Dlugokencky, E. J., Miller, B. R., Montzka, S. A., Hall, B., Neff, W., Sweeney, C., Turnbull, J. C., Wolfe, D. E., Tans, P. P., Gurney, K. R., and Guilderson, T. P.: Constraints on emissions of carbon monoxide, methane, and a suite of hydrocarbons in the Colorado Front Range using observations of $^{14}CO_2$, Atm. Chem. Phys., 13, 11101-11120, doi:10.5194/acp-13-11101-2013, 2013.
Levin, I., Kromer, B., Schmidt, M., and Sartorius, H.: A novel approach for independent budgeting of fossil fuel CO_2 over Europe by $^{14}CO_2$ observations, Geophys. Res. Lett., 30, 2194, 10.1029/2003gl018477, 2003.
Levin, I., Naegler, T., Kromer, B., Diehl, M., Francey, R. J., Gomez-Pelaez, A. J., Steele, L. P., Wagenbach, D., Weller, R., and Worthy, D. E.: Observations and modelling of the global distribution and long-term trend of atmospheric $^{14}CO_2$, Tellus B, 62, 26-46, 10.1111/j.1600-0889.2009.00446.x, 2010.
Levin, I., and Karstens, U. T. E.: Inferring high-resolution fossil fuel CO_2 records at continental sites from combined $^{14}CO_2$ and CO observations, Tellus B, 59, 245-250, 10.1111/j.1600-0889.2006.00244.x, 2007.
Levin, I., and Rödenbeck, C.: Can the envisaged reductions of fossil fuel CO_2 emissions be detected by atmospheric observations?, Naturwissenschaften, 95, 203-208, 10.1007/s00114-007-0313-4, 2007.
Loh, Z., Leuning, R., Zegelin, S., Etheridge, D., Bai, M., Naylor, T., and Griffith, D.: Testing Lagrangian atmospheric dispersion modelling to monitor CO_2 and CH_4 leakage from geosequestration, Atm. Env., 43, 2602-2611, 10.1016/j.atmosenv.2009.01.053, 2009.
Meijer, H. A. J., Smid, H. M., Perez, E., and Keizer, M. G.: Isotopic characterization of anthropogenic CO_2 emissions using isotopic and radiocarbon analysis, Physical Chemistry of the Earth, 21, 483-487, 1996.
Miller, J. B., Lehman, S. J., Montzka, S. A., Sweeney, C., Miller, B. R., Wolak, C., Dlugokencky, E. J., Southon, J. R., Turnbull, J. C., and Tans, P. P.: Linking emissions of fossil fuel CO_2 and other anthropogenic trace gases using atmospheric $^{14}CO_2$, J. Geophys. Res., 117, D08302, 10.1029/2011JD017048, 2012.
Nisbet, E., and Weiss, R.: Top-Down Versus Bottom-Up, Science, 328, 1241-1243, 10.1126/science.1189936, 2010.
NZMED: New Zealand's Energy Outlook 2010, New Zealand Ministry of Economic Development, Wellington, New Zealand, 2010.

Palstra, S. W. L., Karstens, U., Streurman, H.-J., and Meijer, H. A. J.: Wine ethanol ^{14}C as a tracer for fossil fuel CO_2 emissions in Europe: Measurements and model comparison, J. Geophys. Res., 113, D21305, 10.1029/2008jd010282, 2008.

Pasquill, F.: The estimation of the dispersion of windborne material, The meteorological magazine, 90, 33-49, 1961.

Randerson, J. T.: Seasonal and latitudinal variability of troposphere $\Delta^{14}CO_2$: Post bomb contributions from fossil fuels, oceans, the stratosphere, and the terrestrial biosphere, Global Biogeochem. Cycles, 16, 1112, 10.1029/2002gb001876, 2002.

Riley, W. J., Hsueh, D. Y., Randerson, J. T., Fischer, M. L., Hatch, J. G., Pataki, D. E., Wang, W., and Goulden, M. L.: Where do fossil fuel carbon dioxide emissions from California go? An analysis based on radiocarbon observations and an atmospheric transport model, J. Geophys. Res., 113, G04002, 10.1029/2007jg000625, 2008.

Roberts, A., and Thomson, N.: Seasonal distribution of pasture production in New Zealand XVII. South Taranaki, New Zealand Journal of Experimental Agriculture, 12, 83-92, 1984.

Ryerson, T. B., Trainer, M., Holloway, J., Parrish, D. D., Huey, L., Sueper, D., Frost, G. J., Donnelly, S., Schauffler, S., Atlas, E., Kuster, W., Golden, P., Hubler, G., Meagher, J., and Fehsenfeld, F.: Observations of ozone formation in power plant plumes and implications for ozone control strategies, Science, 292, 719-723, 2001.

Shibata, S., Kawano, E., and Nakabayashi, T.: Atmospheric $[^{14}C]CO_2$ variations in Japan during 1982–1999 based on ^{14}C measurements of rice grains, Applied Radiation and Isotopes, 63, 285-290, 10.1016/j.apradiso.2005.03.011, 2005.

Stuiver, M., and Polach, H. A.: Discussion: Reporting of ^{14}C data, Radiocarbon, 19, 355-363, 1977.

Suess, H. E.: Radiocarbon concentration in modern wood, Science, 122, 414-417, 1955.

Tans, P. P., De Jong, A. F., and Mook, W. G.: Natural atmospheric ^{14}C variation and the Suess effect, Nature, 280, 826-828, 1979.

Tans, P. P., Fung, I. Y., and Takahashi, T.: Observational constraints on the global atmospheric CO_2 budget, Science, 247, 1431-1438, 1990.

Thornton, P., Law, B. E., Gholz, H. L., Clark, K. L., Falge, E., Ellsworth, D., Goldstein, A. H., Monson, R. K., Hollinger, D., Falk, M., Chen, J. M., and Sparks, J.: Modeling and measuring the effects of disturbance history and climate on carbon and water budgets in evergreen needleleaf forests, Agricultural and Forest Meteorology, 113, 185-222, 2002.

Thornton, P., Running, S., and Hunt, E.: Biome-BGC: Terrestrial Ecosystem Process Model, Version 4.2. Data model. , Numerical Terradynamic Simulation Group, School of Forestry, University of Montana, Missoula, Montana, USA, 2005.

Trainer, M., Ridley, B., Buhr, M., Kok, G., Walega, J., Hübler, G., Parrish, D. D., and Fehsenfeld, F.: Regional ozone and urban plumes in the southeastern United States: Birmingham, a case study, J. Geophys. Res., 100, 18823-18834, 1995.

Turnbull, J. C., Karion, A., Fischer, M. L., Faloona, I., Guilderson, T., Lehman, S. J., Miller, B. R., Miller, J. B., Montzka, S., Sherwood, T., Saripalli, S., Sweeney, C., and Tans, P. P.: Assessment of fossil fuel carbon dioxide and other anthropogenic trace gas emissions from airborne measurements over Sacramento, California in spring 2009, Atm. Chem. Phys., 11, 705-721, 10.5194/acp-11-705-2011, 2011a.

Turnbull, J. C., Tans, P. P., Lehman, S. J., Baker, D., Chung, Y., Gregg, J. S., Miller, J. B., Southon, J. R., and Zhao, L.: Atmospheric observations of carbon monoxide and fossil

fuel CO_2 emissions from East Asia, J. Geophys. Res., 116, D24306, 10.1029/2011JD016691, 2011b.

Turnbull, J. C., Rayner, P. J., Miller, J. B., Naegler, T., Ciais, P., and Cozic, A.: On the use of $^{14}CO_2$ as a tracer for fossil fuel CO_2: quantifying uncertainties using an atmospheric transport model, J. Geophys. Res., 114, D22302, 10.1029/2009JD012308, 2009.

Turnbull, J. C., Lehman, S. J., Miller, J. B., Sparks, R. J., Southon, J. R., and Tans, P. P.: A new high precision $^{14}CO_2$ time series for North American continental air, J. Geophys. Res., 112, D11310, doi:10.1029/2006JD008184, 2007.

Turnbull, J. C., Miller, J. B., Lehman, S. J., Tans, P. P., Sparks, R. J., and Southon, J. R.: Comparison of $^{14}CO_2$, CO and SF_6 as tracers for determination of recently added fossil fuel CO_2 in the atmosphere and implications for biological CO_2 exchange, Geophys. Res. Lett., 33, L01817, 10.1029/2005GL024213, 2006.

Ummel, K.: CARMA revisited: an updated database of carbon dioxide emissions from power plants worldwide, Center for Global Development, Washington, D.C., 2012.

USEPA: 2008 National Emissions Inventory, version 2 Technical Support Document, US Environmental Protection Agency, Office of Air Quality Planning and Standards, Air Quality Assessment Division, Research Triangle Park, North Carolina, 2012.

Van Der Laan, S., Karstens, U., Neubert, R. E. M., Van Der Laan-Luijkx, I. T., and Meijer, H. A. J.: Observation-based estimates of fossil fuel-derived CO_2 emissions in the Netherlands using $\Delta^{14}C$, CO and ^{222}Radon, Tellus B, 62, 389-402, 10.1111/j.1600-0889.2010.00493.x, 2010.

Vogel, F. R., Hammer, S., Steinhof, A., Kromer, B., and Levin, I.: Implication of weekly and diurnal ^{14}C calibration on hourly estimates of CO-based fossil fuel CO_2 at a moderately polluted site in southwestern Germany, Tellus B, 62, 512-520, 10.1111/j.1600-0889.2010.00477.x, 2010.

Wheeler, D., and Ummel, K.: Calculating CARMA: global estimation of CO_2 emissions from the power sector, Center for Global Development, Washington, D.C., 2008.

Wilson, J. D., and Sawford, B. L.: Review of Lagrangian stochastic models for trajectories in the turbulent atmosphere, Boundary-Layer Meteorology, 78, 191-210, 1996.

Figures

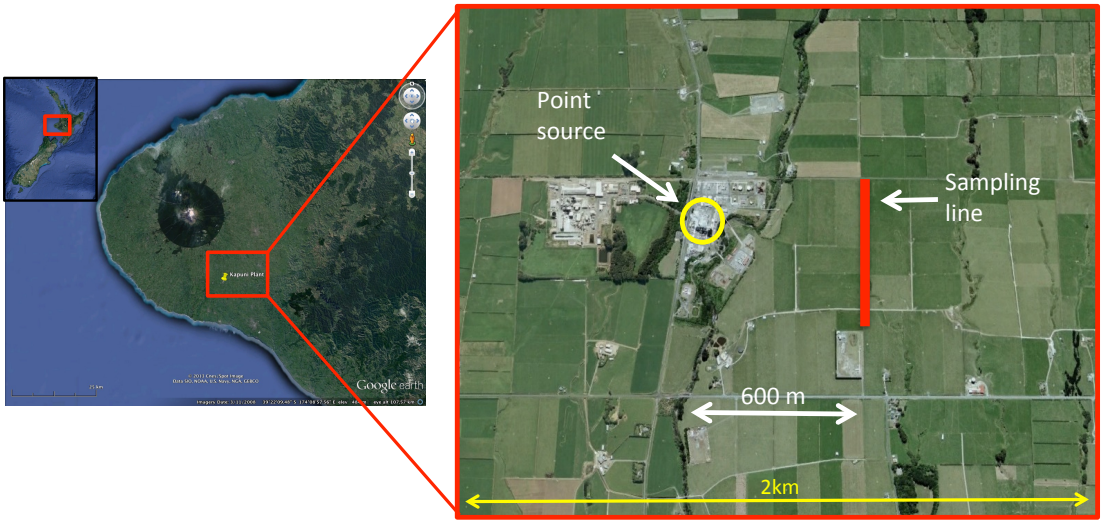

Figure 1. Map showing location of Kapuni processing plant and kite sampling locations.

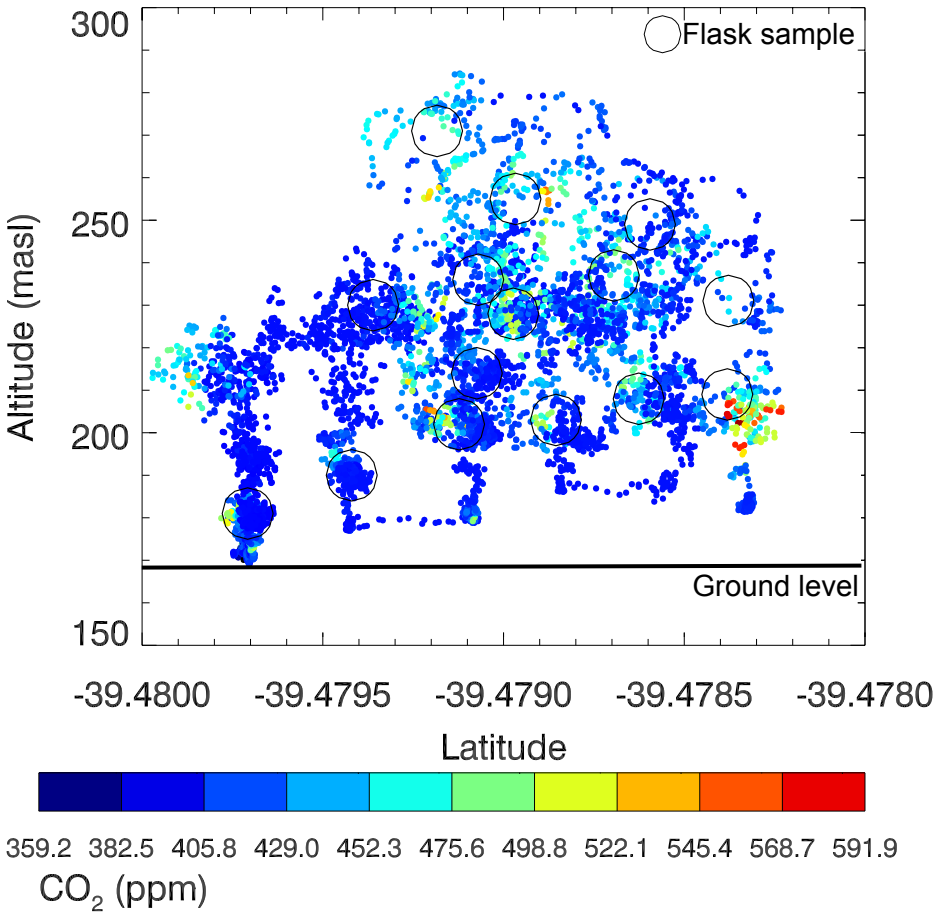

Figure 2. Measured CO_2 mole fraction across transect from south to north. Large black circles indicate the flask sampling locations.

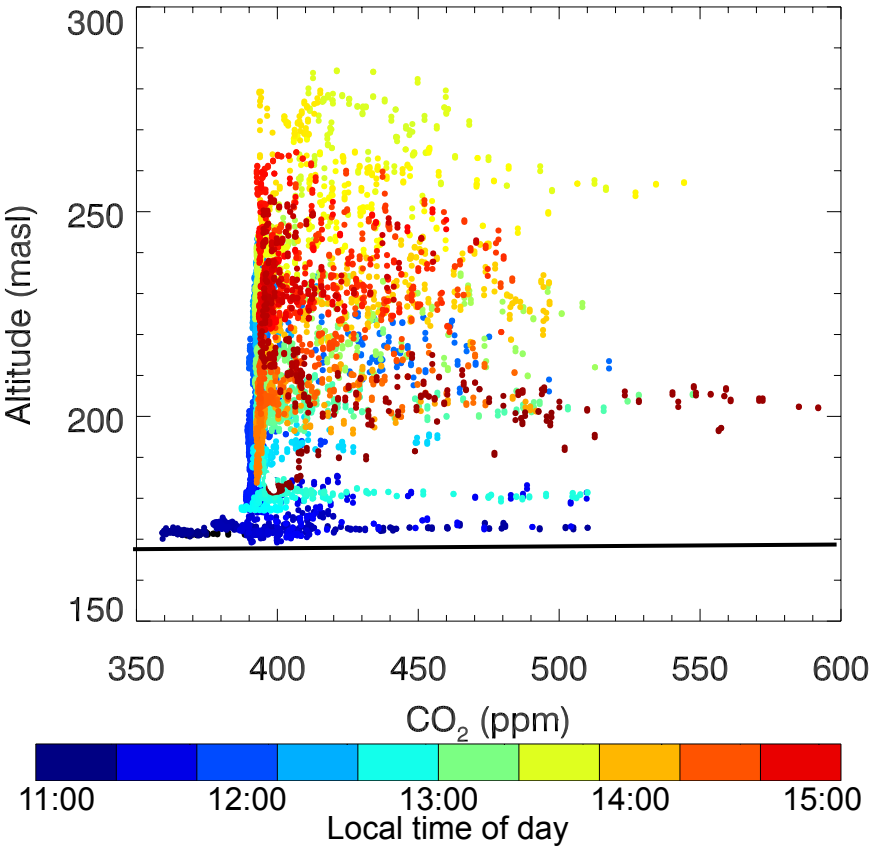

Figure 3. Measured CO_2 mole fraction as a function of altitude. Colours indicate the time of day.

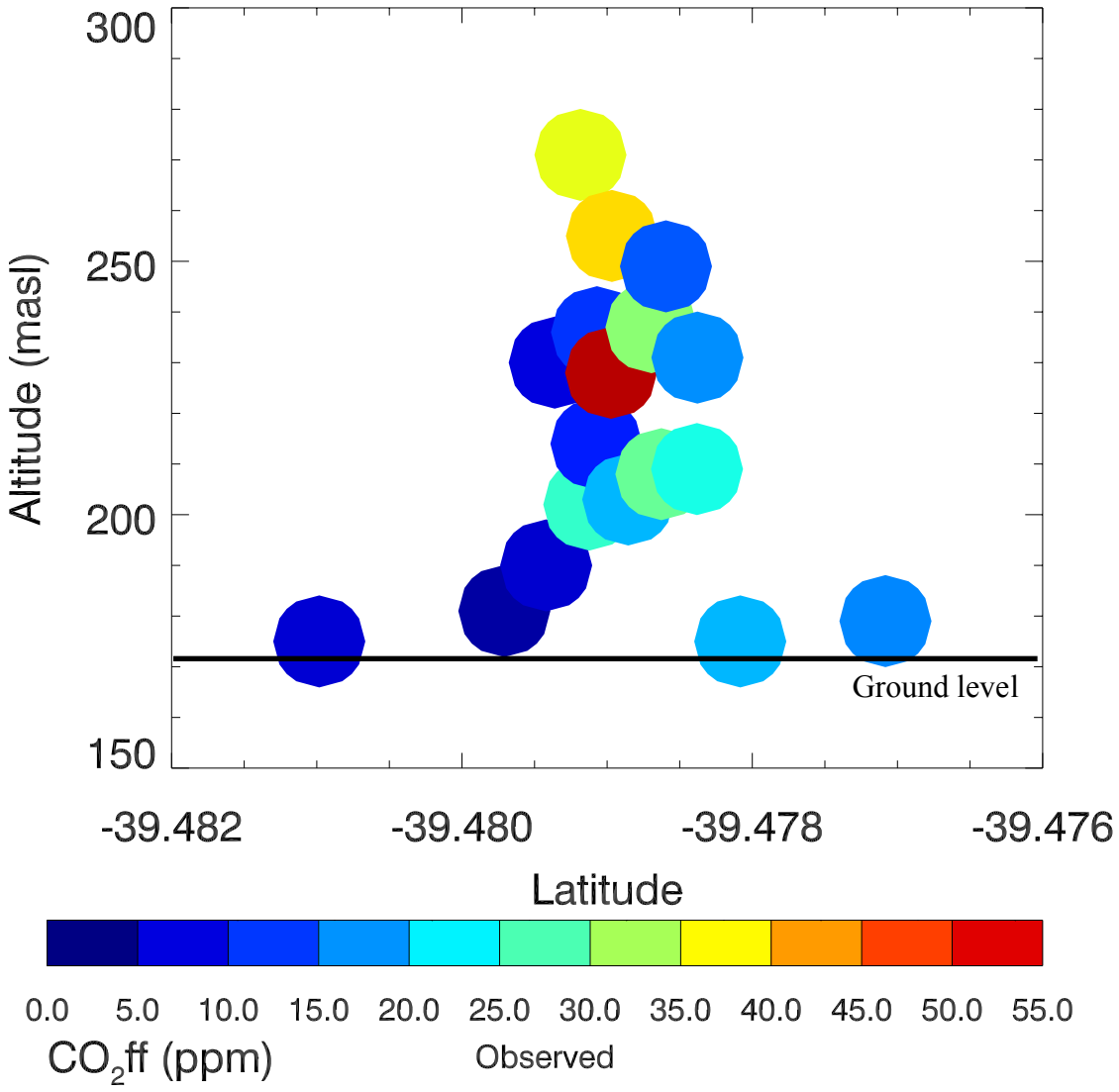

Figure 4. CO_2ff calculated from flask samples from the Helikite and surface flasks on October 26th, 2013.

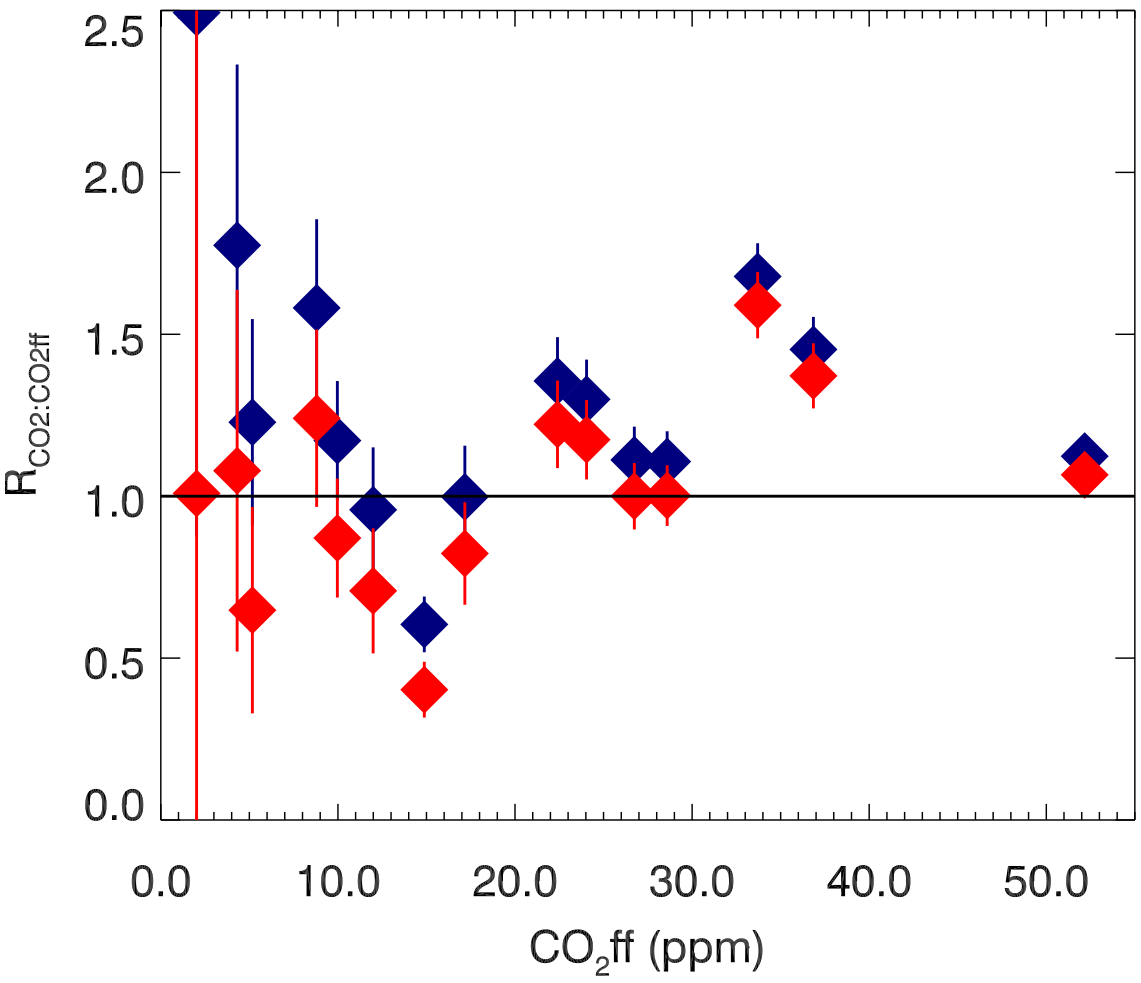

Figure 5. $R_{CO2:CO2ff}$ in each flask sample. Blue points use the assigned CO_2 background values, red points apply a 3 ppm bias to the CO_2 background values in calculating $R_{CO2:CO2ff}$.

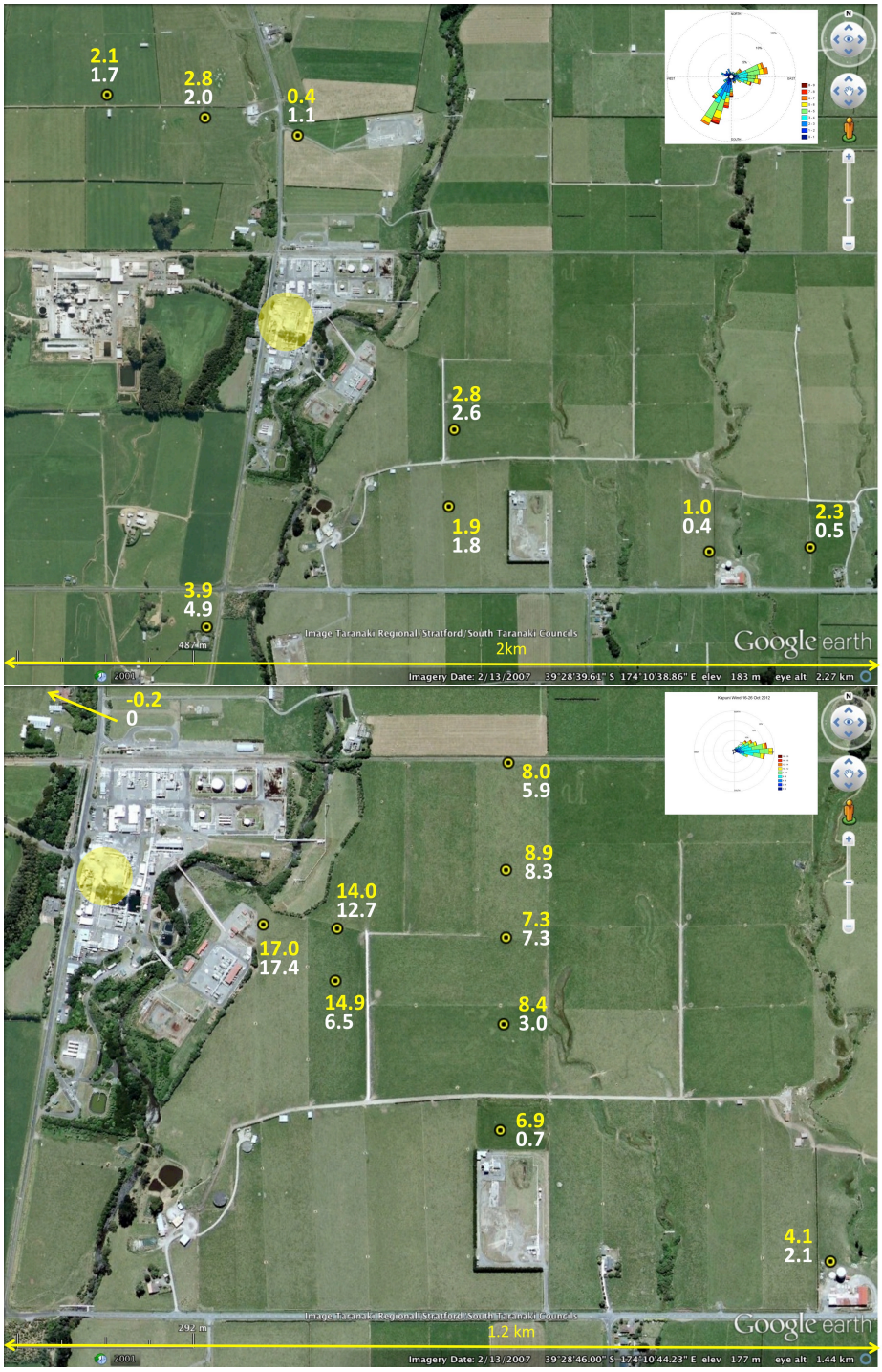

Figure 6. CO_2ff in grass samples collected on August 14th, 2012 (top) and October 24th, 2012 (bottom). The observed CO_2ff derived from $\Delta^{14}C$ is shown in yellow, and the modeled CO_2ff prediction is shown in white. Markers indicate the exact sampling location. A wind rose showing the direction of the wind patterns over the previous one week period is inset (bars indicate the direction the wind is traveling to). In the lower panel the point indicated with the arrow was measured 500 m to the north-west, off the map.

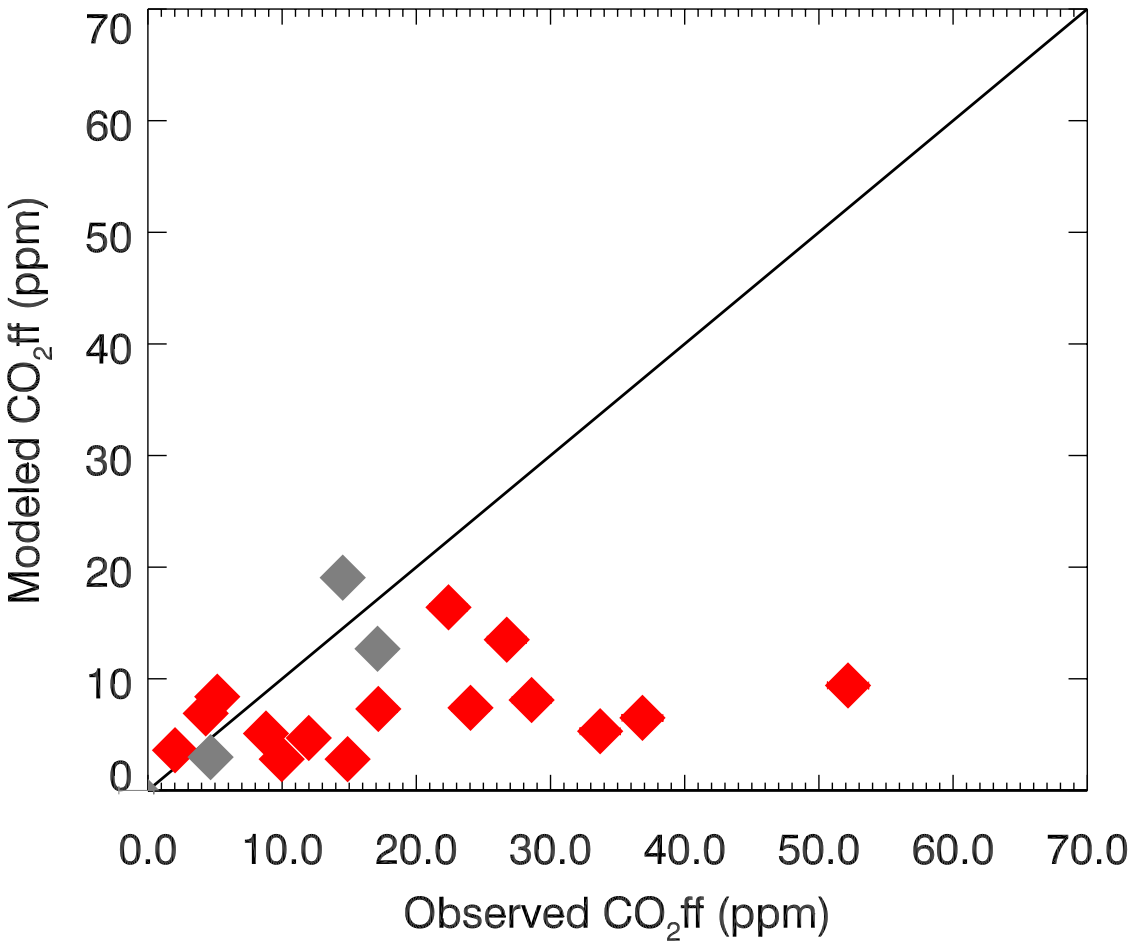

Figure 7. Observed CO_2ff versus modeled CO_2ff for the kite (red) and surface (grey) flask samples. Error bars are omitted for clarity.

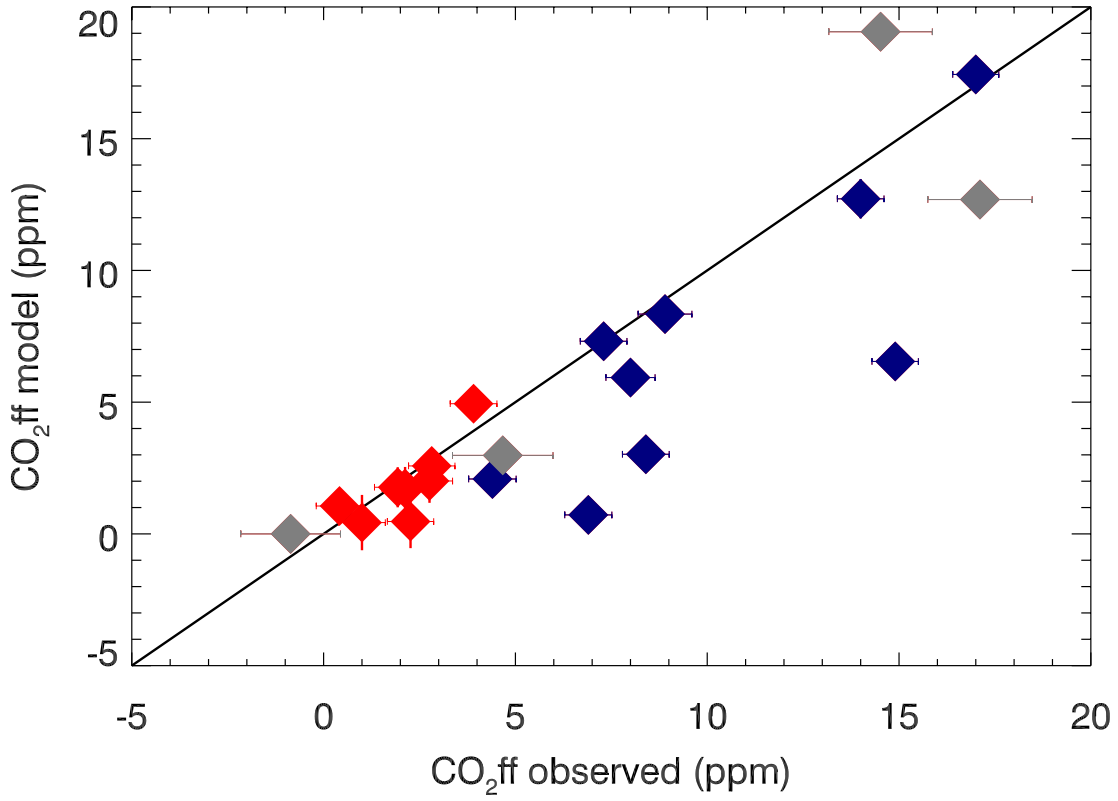

Figure 8. Comparison of observed and modeled CO_2ff from the August (red) and October (blue) grass samples, and October 26th surface flasks (grey). The 1:1 line is shown in black.